

# Inhibition of microRNA-29b suppresses oxidative stress and reduces apoptosis in ischemic stroke

<https://doi.org/10.4103/1673-5374.314319>

Date of submission: July 21, 2020

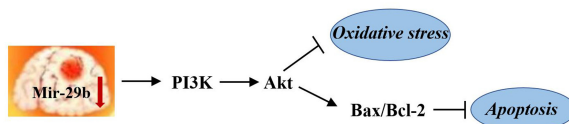
Date of decision: September 14, 2020

Date of acceptance: March 26, 2021

Date of web publication: July 8, 2021

Yao-Hua Ma, Wen-Jing Deng, Zhi-Yi Luo, Jing Jing, Peng-Wei Pan, Yao-Bing Yao, Yan-Bo Fang, Jun-Fang Teng\*

## Graphical Abstract Role of microRNA-29b (miR-29b) in cerebral ischemic injury



## Abstract

MicroRNAs (miRNAs) regulate protein expression by antagonizing the translation of mRNAs and are effective regulators of normal nervous system development, function, and disease. MicroRNA-29b (miR-29b) plays a broad and critical role in brain homeostasis. In this study, we tested the function of miR-29b in animal and cell models by inhibiting miR-29b expression. Mouse models of middle cerebral artery occlusion were established using the modified Zea-Longa suture method. Prior to modeling, 50 nmol/kg miR-29b antagomir was injected via the tail vein. MiR-29b expression was found to be abnormally increased in ischemic brain tissue. The inhibition of miR-29b expression decreased the neurological function score and reduced the cerebral infarction volume and cell apoptosis. In addition, the inhibition of miR-29b significantly decreased the malondialdehyde level, increased superoxide dismutase activity, and Bcl-2 expression, and inhibited Bax and Caspase3 expression. PC12 cells were treated with glutamate for 12 hours to establish *in vitro* cell models of ischemic stroke and then treated with the miR-29 antagomir for 48 hours. The results revealed that miR-29b inhibition in PC12 cells increased Bcl-2 expression and inhibited cell apoptosis and oxidative damage. These findings suggest that the inhibition of miR-29b inhibits oxidative stress and cell apoptosis in ischemic stroke, producing therapeutic effects in ischemic stroke. This study was approved by the Laboratory Animal Care and Use Committee of the First Affiliated Hospital of Zhengzhou University (approval No. 201709276S) on September 27, 2017.

**Key Words:** Akt; apoptosis; cerebral artery occlusion; ischemic stroke; malondialdehyde; microRNA-29b; oxidative stress; PI3K; superoxide dismutase

Chinese Library Classification No. R453; R741.05; Q522

## Introduction

Ischemic cerebrovascular disease is characterized by high morbidity, a high recurrence rate, a high disability rate, and a high mortality rate, which seriously affects human health and life; therefore, the prevention and treatment of ischemic cerebrovascular disease have attracted global attention (Van Broeckhoven et al., 1990). Ischemic encephalopathy is an important cause of severe brain damage. Cerebral ischemic disease plays a major role in cerebrovascular disease, which causes neuronal degeneration, necrosis, or apoptosis and produce an inflammatory response (Feng et al., 2018; Martinez-Coria et al., 2021). At present, the specific mechanism underlying the neurological dysfunction caused by ischemic encephalopathy has not yet been fully studied. Apoptosis and oxidative stress after stroke may represent important molecular mechanisms of ischemic brain disease (Gregório et al., 2019). Therefore, anti-apoptotic or antioxidant agents may be suitable for the treatment of cerebral ischemic injury.

MicroRNAs (miRNAs) are highly conserved, endogenous, small, non-coding RNAs that primarily act to negatively regulate gene expression at the post-transcriptional level (Mott et al., 2010; Ma et al., 2020). One miRNA can regulate multiple messenger RNAs (mRNAs) simultaneously, and one mRNA

can also be regulated by multiple miRNAs simultaneously (Tian et al., 2019). MiRNAs play important regulatory roles in various biological and pathological processes (Gai et al., 2018; Liu et al., 2020). MicroRNA-29b (miR-29b) targets phosphoinositide 3-kinase (PI3K, p85a), insulin-like growth factor-1, and B-Myb to regulate the proliferation of damaged muscle cells, increase the levels of cell cycle arrest proteins, and induce cellular aging in muscles. In a study examining the recovery following meniscus surgery, miR-29b-3p expression in meniscus tissue was shown to increase significantly on day 1 after surgery, followed by a gradual increase over time (Shumnalieva et al., 2017). In addition, low miR-29b expression levels have protective effects against cardiac and liver ischemia-reperfusion injury (Zhong et al., 2019). MiR-29b may also regulate proteins such as Bcl-w and myeloid cell leukemia 1 (Slattery et al., 2017). Bcl-2 protein is a kind of proto-oncogene, which has the effect of inhibiting apoptosis (Saghiri et al., 2017). When neurons in the brain are damaged and undergo apoptosis, the expression of Bcl-2 increases. Therefore, we explored the role played by miR-29b in cerebral ischemic injury and using *in vivo* and *in vitro* experiments.

## Materials and Methods

### Animals

All experimental mice were male, C57BL/6, specific pathogen-

Neurological Intensive Care Unit, the First Affiliated Hospital of Zhengzhou University, Zhengzhou, Henan Province, China

\*Correspondence to: Jun-Fang Teng, MS, junfangteng@163.com.

<https://orcid.org/0000-0003-3255-1301> (Jun-Fang Teng)

**How to cite this article:** Ma YH, Deng WJ, Luo ZY, Jing J, Pan PW, Yao YB, Fang YB, Teng JF (2022) Inhibition of microRNA-29b suppresses oxidative stress and reduces apoptosis in ischemic stroke. *Neural Regen Res* 17(2):433-439.

free, and aged 6–8 weeks. All mice used in the experiment were obtained from the Animal Experiment Center of the First Affiliated Hospital of Zhengzhou University (license No. 2016-003). All mice were maintained in a cage with constant humidity and temperature and a 12-hour light/dark cycle. Forty-eight mice were randomly divided into four groups: control, middle cerebral artery occlusion (MCAO), MCAO + miR-29b antagomir, and MCAO + antagomir control groups ( $n = 12$ /per group). All mice in the MCAO, MCAO + miR-29b antagomir, and MCAO + antagomir control groups underwent MCAO surgery. Antagomirs are specially labeled and chemically modified single-stranded small RNAs designed to interact with the mature miRNA sequence. Antagomirs are highly effective blockers specifically designed to inhibit endogenous miRNAs. The antagomir control group was treated with a single-stranded, small RNA synthesized using the antagomir negative control sequence in this study. The purpose of this group was to exclude the effects of non-specific responses to antagomir injection on the experimental results. The miR-29b antagomir or antagomir control agent (GenePharma, Shanghai, China) was administered through tail vein injection at a concentration of 50 nmol/kg before the performance of MCAO. All experimental procedures were approved by the Laboratory Animal Care and Use Committee of the First Affiliated Hospital of Zhengzhou University (approval No. 201709276S) on September 27, 2017.

### Establishment of cerebral ischemia model

Before the experiment, mice were fasted for 12 hours and deprived of water for 6 hours. The MCAO mouse model was prepared following the modified Zea-Longa suture method (Ruan et al., 2013), in which 10% chloral hydrate (0.3 mL/100 g, Sigma-Aldrich, St. Louis, MO, USA) was injected intraperitoneally. After the mice stabilized, they were fixed in place, and the skin was prepared and disinfected. First, the mice were anesthetized and euthanized by intraperitoneal injection of 5 mg/kg sodium pentobarbital (Xinyu, Shanghai, China), then the brain tissues of the mice were taken out for the next step. A carotid midline incision was used to separate the subcutaneous tissue, after which the muscle layer was separated to expose the common carotid artery, external carotid artery, and internal carotid artery. The common carotid artery was separated from the surrounding tissues and clamped. The main trunk of the external carotid artery was ligated at the distal heart. The internal carotid artery was separated and clamped. A small cut was made to the external carotid artery, and a plug was inserted until the internal carotid artery blackened. A Perfusion Speckle Imager (Pari, Starnberg, Germany) was used to monitor the cerebral blood perfusion on both sides to determine whether the model was successfully established (To et al., 2019). The percentage of cerebral blood perfusion on the ischemic side = (left cerebral blood perfusion – right cerebral blood perfusion)/left cerebral blood perfusion  $\times 100$ . A greater than 50% reduction in blood perfusion volume on the affected side was established as the criterion for successful embolization (Ansson et al., 2018). Mice were subjected to 2 hours of MCAO and then treated with miR-29b antagomir control for 24 hours of reperfusion via the tail vein.

### Nervous system score

We used a modified 6-point scoring system (Côté et al., 1989) to perform neurological assessments on mice 24 hours after MCAO surgery: normal motor function received a score of 0; if the torso and contralateral forelimb were flexible when the mice were lifted by the tail, they received a score of 1; if the mice circled when held by the tail on a flat surface, they received a score of 2; mice that leaning to one side at rest received a score of 3; mice without spontaneous motor activity received a score of 4; and mice that died within 24 hours received a score of 5.

### 2,3,5-Triphenyltetrazolium chloride staining

The mice were anesthetized with 2% pentobarbital before being sacrificed. After the animals were sacrificed by decapitation, the brains were quickly removed (within 10 minutes), placed into 0–4°C phosphate-buffered saline, and frozen at –20°C for 30 minutes. The removed brain tissue was divided into two parts, one part was fresh tissue for fixation, and the other part was frozen and stored. Fresh tissue sections were placed in a small petri dish filled with 2,3,5-triphenyltetrazolium chloride staining solution (Solarbio, Beijing, China) and incubated in a water bath at 37°C for 15–30 minutes in the dark. The color changes in the samples could be observed during the incubating period. The 2,3,5-triphenyltetrazolium chloride solution was removed with a pipette, placed in a separate container, and stored at 4–8°C. The prepared section was washed with prepared tissue washing solution to remove excess staining solution from the tissue surface. At this time, the experimental results could be observed with the naked eye, and images were obtained immediately.

### Immunofluorescence staining

The ischemic part of brain tissue was stained by paraffin. Paraffin sections of brain tissue were dehydrated with ethanol and then dewaxed with xylene. The endogenous peroxidase activity was removed from treatment with 0.03% hydrogen peroxide (or methanol solution: mainly to prevent blood-rich specimens) and incubated at room temperature for 10 minutes. The samples were washed with distilled water once and soaked in phosphate-buffered saline for 5 minutes. Antigen retrieval solution containing 0.4% pepsin (0.4 g pepsin + 0.1 N HCl 100 mL) was preheated to 37°C for 20 minutes. The normal goat serum blocking solution (diluted with phosphate-buffered saline) was added dropwise, stored at room temperature for 20 minutes, and the liquid was shaken off without washing the membrane. A rabbit anti-caspase3 antibody (1:200, Cat# 33915, LI-COR, Lincoln, NE, USA) was added dropwise and incubated overnight at 4°C, and the sections were taken out the next day and reheated at 37°C for 30 minutes. DIPA was added to cover the tissues in each specimen and was incubated at 37°C for half an hour. The membrane was washed with phosphate-buffered saline three times for 5 minutes each time. A goat anti-rabbit IgG labeled with red fluorescein (1:2000, Cat# 925-68070, LI-COR) was added dropwise and incubated at 37°C for 30 minutes. The membrane was washed with phosphate-buffered saline three times for 5 minutes each time. The slides were preserved with glycerin and photographed.

### Cell culture and treatment

We selected the PC12 nerve cell line for this experiment. PC12 cells are a commonly used nerve cell line. PC12 cells are differentiated cells isolated from a rat adrenal medulla pheochromocytoma with the general characteristics of neuroendocrine cells that are widely used in neurophysiological and neuropharmacological research owing to their passage characteristics (Su and Shih, 2015). PC12 cells (American Type Culture Collection, Manassas, VA, USA) were cultured using Dulbecco's modified Eagle medium (Gibco, Winooski, VT, USA) containing 10% fetal bovine serum (Gibco). The cell culture conditions were 37°C in a 5% CO<sub>2</sub> incubator (Gibco). For various experiments, multiple concentrations (12.5, 25, 50, and 100 mM) of glutamic acid (Shanghai Terer Optoelectronics Company, Shanghai, China) were used to treat PC12 cells for various intervention times (4, 8, 12, and 24 hours) according to a previous study (Yu et al., 2020).

### Cell transfection and luciferase assay

Luciferase assays were measured using the Dual-Luciferase<sup>®</sup> Reporter (DLR<sup>™</sup>) Assay System (Promega, Madison, WI, USA), according to the manufacturer's instructions. The luciferase digested nucleic acid fragments were then inserted

into pmirGLO vectors (Solarbio) between NheI and Sall. The co-transfection of pmirGLO plasmids and miRNA mimics (Guangzhou Borui Biotechnology Co., Ltd., Guangzhou, China) in PC12 cells were performed using Lipofectamine 2000 reagent (Invitrogen, Grand Island, NY, USA), according to the manufacturer's instructions. After 48 hours, the luciferase activity was measured.

#### **Real-time fluorescence quantitative polymerase chain reaction**

Before performing real-time fluorescence quantitative polymerase chain reaction, we first used TRIzol reagent (Invitrogen, Grand Island, NY, USA) to extract total RNA from PC12 cells. Reverse transcription was performed on the extracted RNA by Takara's RNA extraction kit, and then the nucleic acid was detected according to quantitative polymerase chain reaction steps (TakaRa, LA, USA). In addition, we also used the Universal Probe Library (UPL) probe (Dongguan Yihe New Material Technology Company, Dongguan, China) to detect mature miR-29b expression (Sunkavalli et al., 2017). The primers used in this quantitative polymerase chain reaction experiments were synthesized at the Beijing Genomics Institution. The primer sequence for miR-29b was as follows: 5'-GTT ATC CAG TGC AGG GTC CGA TTC GCA CTG GAT ACG ACA CAA AC-3'. Each experiment was repeated three times.

#### **Terminal deoxynucleotidyl transferase dUTP nick-end labeling assay**

Terminal deoxynucleotidyl transferase dUTP nick-end labeling (TUNEL) assay was performed to detect apoptotic PC12 cells using the In Situ Cell Death Detection kit (Roche, Basel, Switzerland), according to the manufacturer's instructions. A fluorescence microscope (Olympus, Tokyo, Japan) was used to obtain the images and assess apoptotic cells. TUNEL-positive cells were cells that expressed green fluorescence. Three different fields of view were randomly selected for each specimen for photographing and counting.

#### **Apoptosis assay**

We used Annexin V-fluorescein isothiocyanate (FITC) apoptosis detection kit (Shanghai Yuyan Scientific Instrument Company, Shanghai, China) and flow cytometry to detect cell apoptosis of PC12 cells and cells from brain tissue, following the manufacturer's instructions. First, the cultured cells were digested by trypsin (Parsyscience) and transferred to Eppendorf tubes. The samples were washed twice with phosphate-buffered saline, and 5  $\mu$ L each of FITC and propidium iodide was added, followed by 500  $\mu$ L of phosphate-buffered saline to resuspend the cells. The stained cells were analyzed on a flow cytometer (BD Bioscience, Franklin Lakes, NJ, USA), and at least 10,000 cells were quantified for each sample. In the flow cytometer, blank cells and isotype reference antibodies were used for quality control.

#### **Detection of oxidative stress levels in cells and tissues**

Kits were used to detect malondialdehyde (MDA) levels and superoxide dismutase (SOD) activity in PC12 cells and brain tissue homogenates, according to the manufacturer's instructions. After grinding the brain tissue, the supernatant homogenate was taken. The MDA kit was purchased from Abcam, and the SOD kit was purchased from Amyjet Technology Co., Ltd., Wuhan, China.

#### **Western blot assay**

Whole protein lysates were extracted from PC12 cells and hippocampus using ice-cold radioimmunoprecipitation assay (RIPA) buffer. Then, the lysed cells or tissues were centrifuged at 12,000  $\times$  g at 4°C for 30 minutes, and the supernatant was removed as the whole protein solution. The protein concentration was measured using the bicinchoninic acid (BCA) protein assay kit (KeyGen BioTech, Nanjing, China).

Proteins were separated by 10% sodium dodecyl sulfate-polyacrylamide gel electrophoresis and transferred to a polyvinylidene difluoride (PVDF) membrane. The PVDF membranes were incubated with 5% skimmed milk powder for 2 hours to block non-specific binding sites. The membrane was then incubated at 4°C overnight with the following primary antibodies: rabbit anti-caspase3 antibody (1:200, Cat# 33915, LI-COR), rabbit anti-PI3K antibody (1:200, Cat# 456-1106, LI-COR), rabbit anti-phospho-(p-)PI3K antibody (1:200, Cat# 23227, LI-COR), rabbit anti-Akt antibody (1:200, Cat# 1620177, LI-COR), rabbit anti-p-Akt antibody (1:200, Cat# 2500, Cell Signaling Technology, Danvers, MA, USA), rabbit anti- $\beta$ -actin antibody (1:4000, Cat# 35569, Thermo Fisher, Waltham, MA, USA), rabbit anti-Bax antibody (1:500, ProteinTech, Wuhan, China), rabbit anti-Bcl2 antibody (1:500, ProteinTech), and rabbit anti-superoxide dismutase-1 (SOD-1) antibody (1:1000, Cat# 28106; Qiagen, Hilden, Germany). The PVDF membrane was washed three times with Tris-buffered saline-Tween-20, and the membrane was incubated with goat anti-rabbit IgG (1:2000, Cat# 925-68070, LI-COR) for 1 hour at room temperature. After the secondary antibody incubation, the membrane was washed three times with Tris-buffered saline-Tween-20 and developed with enhanced chemiluminescence reagents (BD Bioscience). A Laboratories instrument (Olympus) was used to measure the intensity of the band and obtain images.

#### **Statistical analysis**

SPSS 21.0 software (IBM, Armonk, NY, USA) was used for all data analysis. All values in the experiment were recorded as the mean  $\pm$  standard deviation (SD). The Student's *t*-test was used for comparison between two groups.  $P < 0.05$  was considered significant.

## **Results**

### **MiR-29b expression is increased in cerebral ischemia mouse brain tissue and glutamate-treated PC12 cells**

To determine the role of miR-29b in ischemic brain disease, we established a model of ischemic encephalopathy in mice and tested the expression of miR-29b in ischemic brain tissue. The expression level of miR-29b in the MCAO group was significantly increased compared with that in the control group 24 hours after MCAO ( $P = 0.01$ ; **Figure 1A**). We verified this result using an *in vitro* experiment. We used a model of glutamate-induced neuronal PC12 cell damage, which showed that miR-29b expression in glutamate-treated cells was significantly increased compared with that in the control group after 12 hours of glutamate treatment at a concentration of 0, 12.5, 25, 50, and 100 mM, respectively ( $P = 0.02$ ; **Figure 1B**).

### **High expression of miR-29b promotes the glutamate-induced apoptosis of PC12 cells**

To further explore the effects of highly expressed miR-29b on the specific function of cerebral ischemic nerve cells, we overexpressed or inhibited miR-29b in PC12 cells and examined cell apoptosis. First, in preliminary experiments, we found that PC12 cells treated with miR-29b mimics or 24 hours showed the most obvious apoptosis characteristics (TUNEL-positive cells). Therefore, we chose the 24-hour time point for the following experiment. We used flow cytometry to detect apoptosis, and the results showed that miR-29b mimics increased the percentage of apoptosis induced by glutamic acid in PC12 cells ( $P < 0.05$ ). The miR-29b inhibitor was able to reduce glutamate-induced apoptosis in PC12 cells (**Figure 2A and B**). We also used the TUNEL assay to detect apoptosis in PC12 cells and found that miR-29b mimics induced apoptosis in PC12 cells, whereas miR-29b inhibitors decreased PC12 cell apoptosis (**Figure 2C**). In summary, the above experimental results indicated that miR-29b overexpression in cerebral ischemic diseases could promote glutamate-induced apoptosis.

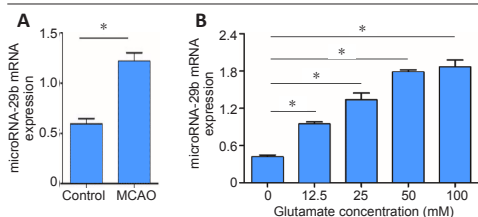


**Figure 1 | MiR-29b expression increases in cerebral ischemia mouse brain tissue and glutamate-treated PC12 cells.**

(A) Real-time polymerase chain reaction detection of miR-29b levels in the whole brain of MCAO mice after 24 hours of reperfusion ( $n = 6$  in each group). (B) Glutamate-induced miR-29b expression in PC12 cells. PC12 cells were seeded on 12-well plates in complete medium for 24 hours prior to 12-hour exposure to glutamate at different concentrations (0, 12.5, 25, 50, 100 mM). Each experiment was repeated three times. Data are represented as the mean  $\pm$  SD. \* $P < 0.05$  (Student's  $t$ -test). MCAO: Middle cerebral artery occlusion; miR-29b: microRNA-29b.

**Downregulation of miR-29b reduces oxidative stress induced by glutamate in PC12 cells**

Oxidative stress is an important mechanism in cerebral ischemic diseases. SOD and MDA are key indicators used to evaluate the level of oxidative stress in cells (Li et al., 2017b). Therefore, we detected the expression of SOD and MDA in the ischemic brain tissue of mice and a cell model of cerebral ischemia in this study. The results showed that MDA [a lipid peroxidation marker (Tsikas, 2017)] level in PC12 cells treated with the miR-29b mimic was significantly increased compared with that in the control group ( $P < 0.05$ ), while MDA level in PC12 cells treated with the miR-29b inhibitor was slightly decreased compared with that in the control group ( $P > 0.05$ ; **Figure 3A**). The SOD activity of PC12 cells treated with miR-29b mimics was significantly decreased compared with that of the control group ( $P < 0.05$ ), while the SOD activity of PC12 cells treated with miR-29b inhibitor was slightly decreased compared with that of the control group ( $P > 0.05$ ; **Figure 3B**). We also examined the expression level of the oxidative stress-related protein SOD-1. The SOD-1 protein expression level in the miR-29b mimic-treated group was significantly lower than that of the control group, and the SOD-1 protein expression level in the miR-29b inhibitor-treated group was higher than that of the control group (all  $P < 0.05$ ; **Figure 3C and D**). These results revealed that miR-29b might be involved in the regulation of oxidative stress in nerve cells under conditions of cerebral ischemic disease.

**Inhibition of miR-29b expression alleviates neurological deficits in mice after cerebral ischemia**

To further investigate the potential role played by miR-29b in cerebral ischemic diseases, we established a mouse cerebral ischemic disease model. We used an miR-29b antagomir to inhibit miR-29b expression in mice and then established a mouse cerebral ischemia model, followed by the detection of the neurological functions of mice after ischemia. The results showed that compared with the control group, the relative mRNA expression of miR-29b in the MCAO group was significantly increased ( $P < 0.05$ ; **Figure 4A**). Neurological scoring was performed after 24 hours of cerebral ischemia in mice. The neurological score of the MCAO group was significantly increased compared with that in the control group and the neurological score of miR-29b-antagomir group was significantly lower than that of MCAO group ( $P < 0.05$ ; **Figure 4B**). We also found that the cerebral infarct size in the MCAO + miR-29b antagomir group was significantly decreased compared with that in the MCAO group ( $P < 0.05$ ; **Figure 4C and D**). Therefore, these experiments indicated that inhibiting the expression of miR-29b in cerebral ischemic diseases may alleviate the neurological symptoms associated with cerebral ischemic diseases. No differences were observed between the

MCAO + antagomir control group and the control group ( $P > 0.05$ ); therefore, the MCAO + antagomir control group was not included in **Figure 4**.

**Inhibition of miR-29b reduces apoptosis in brain tissue cells in cerebral ischemic mice**

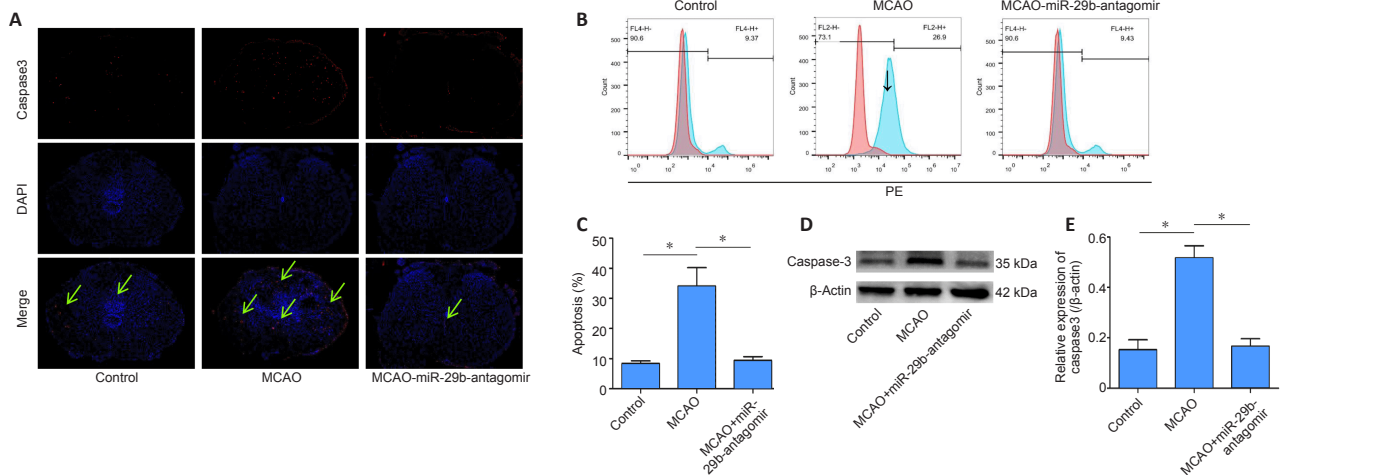
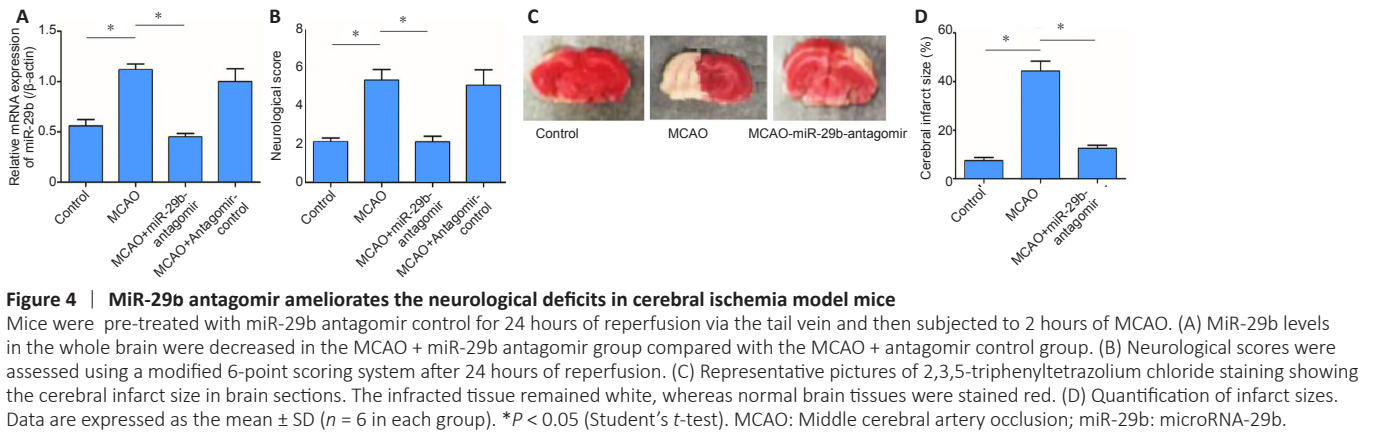
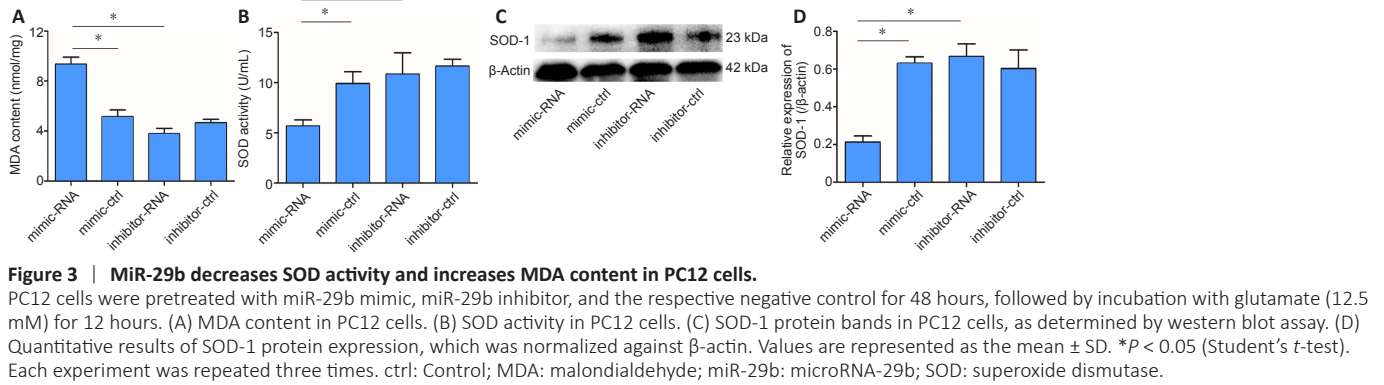
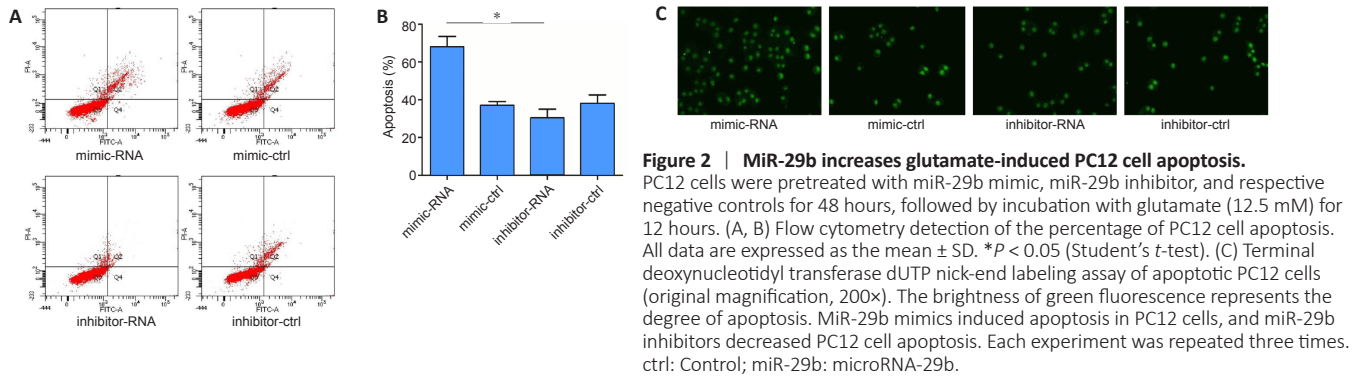
Caspase3 protein is a protein representing cell apoptosis. We used immunofluorescence staining to stain brain tissue sections for caspase3 protein. We found that the number of apoptotic cells in the brain tissue of mice treated with the miR-29b antagomir was significantly decreased compared with that in the MCAO group. The immunopositivity of Caspase3 protein in the brain tissue of the MCAO group was significantly higher than that of the control group, whereas the level of Caspase3 in the CAO-miR-29b-antagomir group was significantly decreased than that of the control group (**Figure 5A**). We removed the brain tissue from the mice and used flow cytometry to detect the percentage of apoptotic cells. We also found that the percentage of apoptotic cells in the MCAO + miR-29b antagomir group was significantly decreased compared with that in the MCAO group ( $P < 0.05$ ; **Figure 5B and C**). We used the western blot assay to detect the expression of apoptotic proteins in the brain tissue of mice. Caspase3 protein expression in the MCAO + miR-29b antagomir group was significantly lower than that in the MCAO group ( $P < 0.05$ ; **Figure 5D and E**). No significant difference was observed between the MCAO + antagomir control group and the control group ( $P > 0.05$ ); therefore, the MCAO + antagomir control group was not included in **Figure 5**.

**Downregulation of miR-29b upregulates antioxidant activity in MCAO mice**

We examined the effects of miR-29b expression on the level of oxidative stress in the brain tissue of cerebral ischemic mice. The results showed that the MDA level in the brain tissue of the MCAO group was significantly increased compared with that of the control group ( $P < 0.05$ ). The MDA level of mice in the MCAO + miR-29b antagomir group was significantly decreased compared with that in MCAO + antagomir control group ( $P < 0.05$ ; **Figure 6A**). The SOD activity of the brain tissue of the MCAO group was significantly decreased compared with that of the control group, whereas the SOD activity of the MCAO + miR-29b antagomir group was significantly increased compared with that of the MCAO group (all  $P < 0.05$ ; **Figure 6B**). Western blot analysis was used to detect the expression of SOD-1 in the brain tissue of mice, which revealed that the level of SOD-1 protein in the brain tissue of the MCAO group was lower than that of the control group ( $P < 0.05$ ). The level of SOD-1 protein in the MCAO + miR-29b antagomir group was significantly higher than that in the MCAO + antagomir control group ( $P < 0.05$ ; **Figure 6C and D**).

**MiR-29b regulates PI3K/Akt/Bax signaling pathway in MCAO mice**

To explore the specific mechanisms through which miR-29b regulates cerebral ischemic cell apoptosis, we further examined changes in apoptosis-related pathways. We examined the PI3K/Akt/Bax signaling pathway in MCAO mice by western blot analysis. The miR-29b antagomir treatment promoted the activation of the PI3K/Akt signaling pathway in the brain tissue of cerebral ischemic mice (**Figure 7A–C**). Treatment with the miR-29b antagomir promoted the expression of the apoptotic protein Bax and inhibited the expression of the anti-apoptotic protein Bcl-2 (**Figure 7A and D**). These results suggested that miR-29b may promote apoptosis and oxidative stress levels in the brain tissues of cerebral ischemic mice by regulating the PI3K/Akt/Bax signaling pathway.



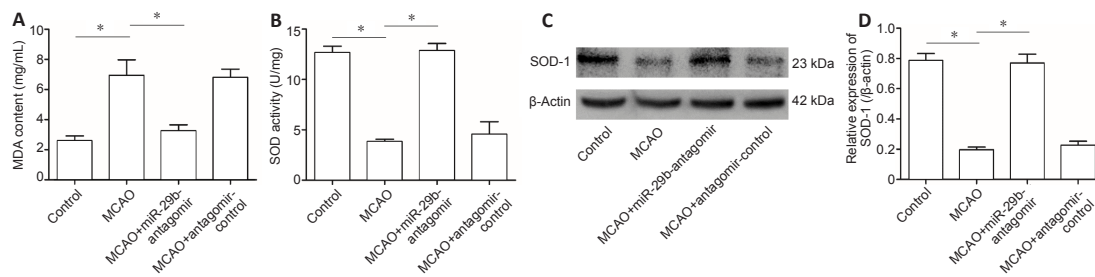


**Figure 6 | MiR-29b upregulates antioxidant systems in mouse brain tissues following cerebral ischemia.** (A, B) Quantitative results for MDA content and SOD activity in the whole brain. (C) Bands of SOD-1 protein detected by western blot assay. (D) Quantitative results for SOD-1 protein expression, which was normalized to β-actin. Data are represented as the mean ± SD (*n* = 6 in each group). \**P* < 0.05 (Student's *t*-test). miR-29b: MicroRNA-29b; MCAO: middle cerebral artery occlusion; MDA: malondialdehyde; SOD: superoxide dismutase.

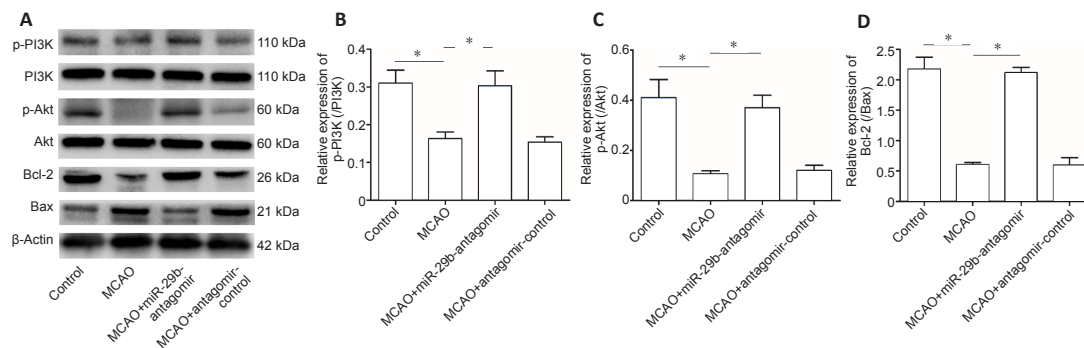


**Figure 7 | MiR-29b regulates the PI3K/Akt/Bax signaling pathway in MCAO model mice.** (A) Bands of protein in the PI3K/Akt/Bax signaling pathway detected by western blot assay. (B) Quantitative results of protein levels for p-PI3K/PI3K (B), p-Akt/Akt (C), and Bcl-2/Bax (D) in the whole brain. Data are presented as the mean ± SD (*n* = 6 in each group). \**P* < 0.05 (Student's *t*-test). MCAO: Middle cerebral artery occlusion; miR-29b: microRNA-29b; PI3K: phosphoinositide 3-kinase.

## Discussion

Neuronal damage after cerebral ischemia is closely related to oxidative stress and mitochondrial dysfunction in nerve cells, which may eventually trigger the apoptotic cascade (Wang et al., 2005). Although researchers have conducted various studies to explore the molecular basis of nerve cell damage following cerebral ischemia, the specific mechanism underlying nerve cell apoptosis after cerebral ischemia has not yet been fully clarified (Liang et al., 2008). The damage that occurs to neurons in the brain after cerebral ischemia may be related to an increase in apoptosis, which may be associated with the expression of Bax and Bcl-2 (Li et al., 2017a; Song et al., 2018). This study found that increased neuronal apoptosis was observed following cerebral ischemia in mouse brain tissues, which was associated with the significant upregulation of Bax and the significant downregulation of Bcl-2. MiRNAs that are specifically expressed in the nervous system inhibit the transcription or alternative splicing of hundreds of neuronal genes, participating in the maintenance of normal structure and function. Differences in the expression sites of miRNA in the brain may be related to differences in the regulatory functions associated with the differentiation and proliferation of neural stem cells. Disordered miRNA networks have been associated with the occurrence and development of human neurodegenerative diseases. MiR-29b antagomir treatment reduces apoptosis in nerve cells, indicating that the neuroprotective effects of the miR-29b antagomir may be achieved through an increase in the expression level of Bcl-2. In addition, oxidative stress may also be an important mechanism of cerebral nerve injury after cerebral ischemia (Guo et al., 2019). The use of antioxidants or the upregulation of antioxidant enzyme activities during cerebral ischemia improves neurological deficits and reduces neuronal cell damage (Malejane et al., 2017). This study showed that the miR-29b antagomir could increase SOD activity and decrease MDA levels significantly in ischemic brain tissue. All of these data indicated that the miR-29b antagomir could promote

cerebral ischemic protection by reducing oxidative stress. Bcl-2 protein is a key protein molecule involved in central nervous system development and apoptosis after DNA damage (Arbour et al., 2008). MiR-29b participates in the occurrence of cancer by regulating changes in related target genes, including the proliferation cycle of cancer cells and the occurrence of apoptosis (Espinosa-Parrilla et al., 2014). In addition, miR-29b also participates in the differentiation and proliferation of human neural stem cells (Trompeter et al., 2013). This study found that the inhibition of miR-29b improved the prognosis of nervous system function after cerebral ischemia. MiRNAs are crucial in the formation of spinal cord morphology and function during nervous system development (Tin et al., 2012). In this study, miR-29b was found to partially regulate the PI3K/Akt signaling pathway activation in the brain tissue of cerebral ischemic mice, regulating the downstream apoptotic protein Bax and the expression of the anti-apoptotic protein Bcl-2. In a study on myotubes, miR-29b was shown to inhibit insulin-like growth factor-1 and PI3K (p85a) and promote myotube atrophy (Zhang et al., 2017). However, the *in vivo* therapeutic effects on nervous system function associated with the targeted regulation of miR-29b are also important. MiR-29b regulates genes associated with fiber types and other related targets in the autophagy pathway (Chen et al., 2004). Some miRNAs participate in the regulation of Bcl-2 family proteins. MiR-15b is highly expressed in MCAO disease tissues and is involved in regulating targeted Bcl-2 protein expression (Hakimizadeh et al., 2017). In addition, Bcl-xL mRNA is an anti-apoptotic member of the Bcl-2 family that binds with miR-491-5p. The increase in miR-29b inhibits Bcl-2 and promotes neuronal cell death after ischemic brain injury (Milani et al., 2018). MiRNA targets and regulates the expression of myeloid cell leukemia 1 in tumor cells to induce tumor cell apoptosis (Yu et al., 2017).

This study also has certain limitations. This study found differences in the expression of miR-29b in ischemic brain tissue, which was also associated with changes in the

expression of downstream related proteins. However, no direct evidence exists to demonstrate how miR-29b directly regulates downstream protein expression, and the *in vitro* experiments of this study were conducted in a PC12 cell line rather than a primary cell line. In future studies, we will use primary cell lines to better simulate disease conditions and further examine the regulatory effects of microRNA on differential proteins.

In summary, we determined that the upregulation of miR-29b is an important factor leading to neuronal cell damage after cerebral ischemia in this study. The results showed that miR-29b might have the potential to regulate apoptosis and oxidative stress. In addition, this study has discovered a key role for miR-29b in cerebral ischemic diseases and identified some potential regulatory proteins (the proteins that miR-29b regulates), which might provide new ideas and targets for the treatment of clinical cerebral ischemic diseases. In future research, we will continue to explore how miR-29b specifically regulates protein expression and continue to investigate whether similar effects exist in other brain injury-associated diseases.

**Author contributions:** *Study design and manuscript draft: YHM, JFT; study guidance: JFT; experiment implementation: WJD, ZYL; statistical analysis: JJ, PWP; data interpretation: YBY, YBF. All authors revised the paper critically for intellectual content and approved the final version. All authors agreed to be accountable for the work and to ensure that any questions relating to the accuracy and integrity of the manuscript are investigated and properly resolved.*

**Conflicts of interest:** *The authors declare that they have no conflict of interest.*

**Financial support:** *None.*

**Institutional review board statement:** *The study was approved by the Laboratory Animal Care and Use Committee of the First Affiliated Hospital of Zhengzhou University (approval No. 201709276S) on September 27, 2017.*

**Copyright license agreement:** *The Copyright License Agreement has been signed by all authors before publication.*

**Data sharing statement:** *Datasets analyzed during the current study are available from the corresponding author on reasonable request.*

**Plagiarism check:** *Checked twice by iThenticate.*

**Peer review:** *Externally peer reviewed.*

**Open access statement:** *This is an open access journal, and articles are distributed under the terms of the Creative Commons Attribution-NonCommercial-ShareAlike 4.0 License, which allows others to remix, tweak, and build upon the work non-commercially, as long as appropriate credit is given and the new creations are licensed under the identical terms.*

**Open peer reviewer:** *Ulises Gomez-Pinedo, Hospital Clinico Universitario San Carlos, Spain.*

**Additional file:** *Open peer review report 1.*

## References

Ansson CD, Sheikh R, Dahlstrand U, Hult J, Lindstedt S, Malmström M (2018) Blood perfusion in Hewes tarsoconjunctival flaps in pigs measured by laser speckle contrast imaging. *JPRAS Open* 18:98-103.

Arbour N, Vanderluit JL, Le Grand JN, Jahani-Asl A, Ruzhynsky VA, Cheung EC, Kelly MA, MacKenzie AE, Park DS, Opferman JT, Slack RS (2008) Mcl-1 is a key regulator of apoptosis during CNS development and after DNA damage. *J Neurosci* 28:6068-6078.

Chen C, Harel A, Gorovits R, Yarden O, Dickman MB (2004) MAPK regulation of sclerotic development in Sclerotinia sclerotiorum is linked with pH and cAMP sensing. *Mol Plant Microbe Interact* 17:404-413.

Côté R, Battista RN, Wolfson C, Boucher J, Adam J, Hachinski V (1989) The Canadian Neurological Scale: validation and reliability assessment. *Neurology* 39:638-643.

Espinosa-Parrilla Y, Muñoz X, Bonet C, García N, Venceslá A, Yiannakouris N, Naccarati A, Sieri S, Panico S, Huerta JM, Barricarte A, Menéndez V, Sánchez-Cantalejo E, Dorronsoro M, Brennan P, Duarte-Salles T, As Bueno-de-Mesquita H, Weiderpass E, Lund E, Clavel-Chapelon F, et al. (2014) Genetic association of gastric cancer with miRNA clusters including the cancer-related genes MIR29, MIR25, MIR93 and MIR106: results from the EPIC-EURGAST study. *Int J Cancer* 135:2065-2076.

Feng X, Zhao T, Liu J, Zhou C (2018) Cerebral venous sinus thrombosis with cerebral hemorrhage presenting with status epilepticus in early pregnancy. *Clin Lab* 64:611-614.

Gai YP, Zhao HN, Zhao YN, Zhu BS, Yuan SS, Li S, Guo FY, Ji XL (2018) MiRNA-seq-based profiles of miRNAs in mulberry phloem sap provide insight into the pathogenic mechanisms of mulberry yellow dwarf disease. *Sci Rep* 8:812.

Gregório T, Pipa S, Cavaleiro P, Atanásio G, Albuquerque I, Castro Chaves P, Azevedo L (2019) Original intracerebral hemorrhage score for the prediction of short-term mortality in cerebral hemorrhage: systematic review and meta-analysis. *Crit Care Med* 47:857-864.

Guo SS, Wang Y, Fan QX (2019) Raddeanin A promotes apoptosis and ameliorates 5-fluorouracil resistance in cholangiocarcinoma cells. *World J Gastroenterol* 25:3380-3391.

Hakimizadeh E, Shamsizadeh A, Roohbakhsh A, Arababadi MK, Hajizadeh MR, Shariati M, Fatemi I, Moghadam-Ahmadi A, Bazmandegan G, Rezaeizadeh H, Allahtavakoli M (2017) TRPV1 receptor-mediated expression of Toll-like receptors 2 and 4 following permanent middle cerebral artery occlusion in rats. *Iran J Basic Med Sci* 20:863-869.

Li JF, Zheng SJ, Wang LL, Liu S, Ren F, Chen Y, Bai L, Liu M, Duan ZP (2017a) Glucosylceramide synthase regulates the proliferation and apoptosis of liver cells in vitro by Bcl-2/Bax pathway. *Mol Med Rep* 16:7355-7360.

Li YH, Liu SB, Zhang HY, Zhou FH, Liu YX, Lu Q, Yang L (2017b) Antioxidant effects of celastrol against hydrogen peroxide-induced oxidative stress in the cell model of amyotrophic lateral sclerosis. *Sheng Li Xue Bao* 69:751-758.

Liang HW, Qiu SF, Shen J, Sun LN, Wang JY, Bruce IC, Xia Q (2008) Genistein attenuates oxidative stress and neuronal damage following transient global cerebral ischemia in rat hippocampus. *Neurosci Lett* 438:116-120.

Liu ZG, Li Y, Jiao JH, Long H, Xin ZY, Yang XY (2020) MicroRNA regulatory pattern in spinal cord ischemia-reperfusion injury. *Neural Regen Res* 15:2123-2130.

Ma ZT, Zeng H, Wang DL, Weng J, Feng S (2020) MicroRNA-138-5p regulates chondrocyte proliferation and autophagy. *Zhongguo Zuzhi Gongcheng Yanjiu* 25:674-678.

Malejane DN, Tinyani P, Soundy P, Sultanbawa Y, Sivakumar D (2017) Deficit irrigation improves phenolic content and antioxidant activity in leafy lettuce varieties. *Food Sci Nutr* 6:334-341.

Martinez-Coria H, Arrieta-Cruz I, Cruz ME, López-Valdés HE (2021) Physiopathology of ischemic stroke and its modulation using memantine: evidence from preclinical stroke. *Neural Regen Res* 16:433-439.

Milani D, Bakeberg MC, Cross JL, Clark VW, Anderton RS, Blacker DJ, Knuckey NW, Meloni BP (2018) Comparison of neuroprotective efficacy of poly-arginine R18 and R18D (D-enantiomer) peptides following permanent middle cerebral artery occlusion in the Wistar rat and in vitro toxicity studies. *PLoS One* 13:e0193884.

Mott JL, Kurita S, Cazanave SC, Bronk SF, Werneburg NW, Fernandez-Zapico ME (2010) Transcriptional suppression of mir-29b-1/mir-29a promoter by c-Myc, hedgehog, and NF-kappaB. *J Cell Biochem* 110:1155-1164.

Ruan GP, Han YB, Wang TH, Xing ZG, Zhu XB, Yao X, Ruan GH, Wang JX, Pang RQ, Cai XM, He J, Zhao J, Pan XH (2013) Comparative study among three different methods of bone marrow mesenchymal stem cell transplantation following cerebral infarction in rats. *Neurosci Res* 35:212-220.

Saghiri MA, Asatourian A, Gurel Z, Sorenson CM, Sheibani N (2017) Bcl-2 expression is essential for development and normal physiological properties of tooth hard tissue and saliva production. *Exp Cell Res* 358:94-100.

Shummalieva R, Kachakova D, Monov S, Kaneva R, Choumnaieva-Ivanova V, Kolarov Z, Rashkov R (2017) 317 Dysregulation of mirnas expression levels and disease activity in sle patients. *Lupus Sci Med* 4:A142-A143.

Slattery ML, Herrick JS, Mullany LE, Samowitz WS, Sevens JR, Sakoda L, Wolff RK (2017) The co-regulatory networks of tumor suppressor genes, oncogenes, and miRNAs in colorectal cancer. *Genes Chromosomes Cancer* 56:769-787.

Song Y, Zhong M, Cai FC (2018) Oxcarbazepine causes neurocyte apoptosis and developing brain damage by triggering Bax/Bcl-2 signaling pathway mediated caspase 3 activation in neonatal rats. *Eur Rev Med Pharmacol Sci* 22:250-261.

Su WT, Shih YA (2015) Nanofiber containing carbon nanotubes enhanced PC12 cell proliferation and neurogenesis by electrical stimulation. *Biomed Mater Eng* 26 Suppl 1:S189-195.

Sunkavalli U, Aguilar C, Silva RJ, Sharan M, Cruz AR, Tawk C, Maudet C, Mano M, Eulalio A (2017) Analysis of host microRNA function uncovers a role for miR-29b-2-5p in Shigella capture by filopodia. *PLoS Pathog* 13:e1006327.

Tian Y, Shang Y, Guo R, Chang Y, Jiang Y (2019) Salinity stress-induced differentially expressed miRNAs and target genes in sea cucumbers *Apostichopus japonicus*. *Cell Stress Chaperones* 24:719-733.

Tin AS, Sundar SN, Tran KQ, Park AH, Poindexter KM, Firestone GL (2012) Antiproliferative effects of artemisinin on human breast cancer cells requires the downregulated expression of the E2F1 transcription factor and loss of E2F1-target cell cycle genes. *Anticancer Drugs* 23:370-379.

To C, Rees-Lee JE, Gush RJ, Gooding KM, Cawrse NH, Shore AC, Wilson ADH (2019) Intraoperative tissue perfusion measurement by laser speckle imaging: a potential aid for reducing postoperative complications in free flap breast reconstruction. *Plast Reconstr Surg* 143:287e-292e.

Trompeter HI, Dreesen J, Hermann E, Iwaniuk KM, Hafner M, Renwick N, Tuschi T, Wernet P (2013) MicroRNAs miR-26a, miR-26b, and miR-29b accelerate osteogenic differentiation of unrestricted somatic stem cells from human cord blood. *BMC Genomics* 14:111.

Tsikis D (2017) Assessment of lipid peroxidation by measuring malondialdehyde (MDA) and relatives in biological samples: Analytical and biological challenges. *Anal Biochem* 524:13-30.

Van Broeckhoven C, Haan J, Bakker E, Hardy JA, Van Hul W, Wehnert A, Vegter-Van der Vlis M, Roos RA (1990) Amyloid beta protein precursor gene and hereditary cerebral hemorrhage with amyloidosis (Dutch). *Science* 248:1120-1122.

Wang Q, Sun AY, Simonyi A, Jensen MD, Shelat PB, Rottinghaus GE, MacDonald RS, Miller DK, Lubahn DE, Weisman GA, Sun GY (2005) Neuroprotective mechanisms of curcumin against cerebral ischemia-induced neuronal apoptosis and behavioral deficits. *J Neurosci Res* 82:138-148.

Yu N, Wang Z, Chen Y, Yang J, Lu X, Guo Y, Chen Z, Xu Z (2017) The ameliorative effect of bloodletting puncture at hand twelve Jing-well points on cerebral edema induced by permanent middle cerebral ischemia via protecting the tight junctions of the blood-brain barrier. *BMC Complement Altern Med* 17:470.

Yu S, Xin W, Jiang Q, Li A (2020) Propofol exerts neuroprotective functions by down-regulating microRNA-19a in glutamic acid-induced PC12 cells. *Biofactors* 46:934-942.

Zhang X, Song H, Qiao S, Liu J, Xing T, Yan X, Li H, Wang N (2017) MiR-17-5p and miR-20a promote chicken cell proliferation at least in part by upregulation of c-Myc via MAP3K2 targeting. *Sci Rep* 7:15852.

Zhong X, Huang G, Ma Q, Liao H, Liu C, Pu W, Xu L, Cai Y, Guo X (2019) Identification of crucial miRNAs and genes in esophageal squamous cell carcinoma by miRNA-mRNA integrated analysis. *Medicine (Baltimore)* 98:e16269.

*P-Reviewer: Gomez-Pinedo U; C-Editor: Zhao M; S-Editors: Yu J, Li CH; L-Editors: Giles L, Yu J, Song LP; T-Editor: Jia Y*